Surface Resistance of Superconductors--Examples from Nb - O Systems

F. Palmer

Outline

0. Introduction
1. BCS Resistance
   - Two fluid model
   - Frequency and temperature dependence
   - Mean free path dependence (anomalous skin effect)
2. Residual resistance
   - Resistive losses
   - Tunneling losses
   - Direct phonon generation
3. Effects of Oxygen
   - Room temperature exposure (no effect)
   - Oxidized surfaces heated to 325°C
   - Energy gap
   - Dependence of RF properties on heating temperature

Trapped magnetic flux

Introduction

The observed surface resistance of most superconductors can be written as the sum of two terms.

$$R_{obs} = R_{BCS} + R_{res}$$

The first term is the surface resistance predicted by the BCS theory, {m2,a2} which is roughly proportional to $(\omega^2/T)e^{-\Delta/T}$. The second term is a sample dependent empirical constant called residual resistance which dominates at low temperatures where the BCS resistance approaches zero. Typical values for the residual resistance of clean niobium range from 2 to 100 nΩ, depending mostly on the details of surface preparation.{k5}

This paper is divided into three sections. The first section describes the BCS theory of surface resistance in terms of a simplified two-fluid model. The second section describes several possible causes of residual resistance including normal conducting materials, tunneling across cracks in the surface, and direct generation of phonons by the RF electric field. The last section describes recent experiments having to do with the effects of oxide layers on surface resistance. Layers grown in pure oxygen at room temperature were found to have little or no effect, but if these layers are heated to temperatures near 300°C, they can alter both the BCS resistance and the residual resistance. Heated oxide layers also increase the dependence of the residual resistance on ambient magnetic field.

1. BCS Resistance

This section describes several features of the BCS part of surface resistance in terms of a simplified two-fluid model. The section is divided into 3 subsections. The first one shows that the two-fluid model gives a useful although inexact approximation to the current density in a superconductor as calculated by Mattis and Bardeen. The mathematics is somewhat tedious here, so the important characteristics of the model are listed in the last paragraph of this subsection. The remaining subsections use this model to describe the dependence of the BCS resistance on frequency, temperature, and mean free path.

Two fluid model:

The expression for the current density, J, as a function of the vector potential, A, was calculated by Mattis and Bardeen,{m2} for $\omega \ll T < T_c/2$ as:

$$[1] \qquad J(r,\omega) = \frac{e^2 N_o}{2\pi^2 \hbar c} \int \frac{R[R\cdot A(r')]I(\omega,R,T)e^{-R/l}\,dr'}{R^4}$$

where $R = r-r'$, $R = |R|$, l is the mean free path, and N_o is the density of states, $dN/d|p|$. The superconducting properties are contained in $I(\omega,R,T)$.

$$[2] \qquad I(\omega,R,T) = -i\pi\int_{\Delta-\hbar\omega}^{\Delta}[1-2f(E+\hbar\omega)]\ X\ [g(E)\cos(a\epsilon_2)-i\sin(a\epsilon_2)]\ e^{ia\epsilon_1}dE$$

$$- i\pi\int_{\Delta}^{\infty}\{[1-2f(E+\hbar\omega)]\ X\ [g(E)\cos(a\epsilon_2)-i\sin(a\epsilon_2)]\ e^{ia\epsilon_1}$$

$$-[1-2f(E)]\ X\ [g(E)\cos(a\epsilon_1)-i\sin(a\epsilon_1)]\ e^{ia\epsilon_2}\}\,dE$$

where $\epsilon_1 = (E^2 - \Delta^2)^{1/2}$, $\epsilon_2 = ((E+\hbar\omega)^2 - \Delta^2)^{1/2}$, $g(E) = (E^2+\Delta^2+\hbar\omega E)/\epsilon_1\epsilon_2$, $a = R/hv_f$, v_f is the fermi velocity, and $f(E)$ is the fermi function, $(1+e^{E/T})^{-1}$.

The normal and superfluid parts of this expression may be separated as follows. If $I(\omega,R,T)$ is real, then J is out of phase with the electric field, $E = i(\omega/c)A$, so no dissipation will occur. On the other hand, for a normal metal,

$$[3] \qquad I(\omega,R,T) = -i\pi\hbar\omega e^{-iR\omega/v_f}$$

Upon fourier transforming to real time, the exponential becomes $\delta(t+R/v_f)$, which has the simple interpretation that a delay of R/v_f is required for electrons to travel from r' to the point where the current is measured. For small T and ω, the first integral in [2] reduces to $-\pi/\Delta^2$, which is part of the supercurrent. The second may be rewritten as

$$[4] \qquad I(\omega,R,T) \sim \pi\int_{\Delta}^{\infty}[1-2f(E)][g(E)-1]\ \sin(\alpha(\epsilon_1+\epsilon_2))\ dE$$

$$+i\pi\int_{\Delta}^{\infty}\hbar\omega\ \frac{df(E)}{dE}\ [g(E)+1]\ e^{-i\alpha(\frac{d\epsilon}{dE})\hbar\omega}\ dE$$

$$+i\pi\int_{\Delta}^{\infty}\hbar\omega\ \frac{df(E)}{dE}\ [g(E)-1]\ e^{i\alpha(\epsilon_1+\epsilon_2)}\ dE$$

where derivative approximations have been used for $f(E+\omega)$ and ϵ_2. The first term in [3] is real and represents the supercurrent, which is independent of ω. This term is also much larger than the other two so that the field pattern in the superconductor is determined primarily by just the supercurrent. The second term is similar to [3], except that the fermi velocity has been replaced by $s = dE/dp$ where $E = (\Delta^2+v_f^2(p-p_f)^2)^{1/2}$. The approximation, $E = \Delta + \rho^2/2m^*$ where $\rho = p-p_f$ and $m^* = \Delta/v_f^2$, gives $s = \rho/m^*$. (The mass is anisotropic in the sense that it is more easily accelerated in its direction of motion than in a transverse direction, but much can be explained without taking this into account.) Note also that the number of normal electrons is reduced by a factor of $df/dE \sim (1/T)\ \exp(-\Delta/T)$. The third term in [3] is very strange, but it is always smaller than the second term, and it falls off rapidly for $R > \xi$.

The two fluid model for $T < T_c/2$ may be summarized as follows. The electro-magnetic fields are determined almost entirely by the supercurrent. The supercurrent density and the magnetic field are independent of ω, and, for $l>>\xi$, they are independent of l. The number of normal electrons is relatively small, since it contains a factor of $df/dE \sim (1/T)e^{-\Delta/T}$. The normal electrons have an effective mass, $m^* = \Delta/v_f^2$ and a velocity given by $(p-p_f)/m^*$, where p_f is the fermi momentum. These velocities can be arbitrarily slow near the fermi surface.

Frequency and temperature dependence:

Many approximations use a frequency dependence of ω^2, which comes from the fact that E is proportional to ω. ($\nabla \times E = i(\omega/c)B$. For any linear relation between E and the normal current, J_n, the losses, $J_n \cdot E$, are proportional to E^2.) A correction to the ω^2 dependence arises due from the slow moving "normal electrons" which rarely scatter during a single RF cycle.

A group of electrons having the same speed (s) but traveling in random directions will have a mean time between collisions of $\tau = l/s$ where l is the mean free path. The average velocity, $\langle v \rangle$, is much smaller than s. In the presence of an oscillating electric field, $E\ \exp(-i\omega t)$, the average velocity obeys

$$\frac{d\langle v\rangle}{dt} = \frac{e\,E\,e^{-i\omega t}}{m^*} - \frac{\langle v\rangle}{\tau} \quad , \text{ or } \langle v\rangle = \frac{eE/m^*}{(s/l)-i\omega}\; e^{-i\omega t}$$

If the number of electrons is dn, then the power loss is Re $(J\cdot E^*)/2$:

[5] $$dP = \frac{e^2E^2}{2m^*}\left(\frac{s/l}{\omega^2+(s/l)^2}\right) dn$$

as anticipated, this expression depends on ω for $s < l\omega$; otherwise it has the same form as the standard expression,

[6] $P = \sigma|E|^2/2$ where $\sigma = ne^2\tau/m$.

The losses in the superconductor may be found by integrating over [4] using $dn = N_o(df/dE)\,d\rho$. For simplicity we approximate $df/dE = (1/T)\,e^{-\Delta/T}$ for $\Delta < E < \Delta+h\omega$, and $df/dE = 0$ otherwise.

$$P = \frac{e^2E^2}{2m^*}\,N_o\,\frac{e^{-\Delta/T}}{T}\,2\int_0^{m^*v_t}\frac{\rho/m^*l}{\omega^2+(\rho/m^*l)^2}\,d\rho$$

or

[7] $$P = \frac{e^2E^2l}{2}\,N_o\,\frac{e^{-\Delta/T}}{T}\log\left(1+\left(\frac{v_t}{\omega l}\right)^2\right)$$

Where the thermal velocity, v_t, is defined by $m^*v_t^2/2 = T$.

Table 1 compares formula [7] with detailed calculations from the program by Halbritter.{h1} The formula has been normalized to agree with the program at T = 1 and f = 31.6 Mhz. We have used the same parameters used by Halbritter for niobium, except that a mean free path of 300Å is used. These values are Tc = 9.2, $\Delta(0) = 17.1^*$, $\lambda_L(0) = 360Å$, and $v_f = 290{,}000$m/s. At 4 degrees, we used $\Delta(4) = 17.02^*$ in our formula, in accordance with the BCS theory.

Table 1

Comparison between formula [7] and Halbritter's program.

(Surface resistances in Ohms)

Temp.	Method	31.6 Mhz.	1 Ghz.	10 Ghz.
1°	program	3.45×10^{-15}	1.82×10^{-12}	7.57×10^{-11}
1°	formula	(same)	2.23×10^{-12}	1.41×10^{-10}
2°	program	9.98×10^{-12}	5.70×10^{-9}	2.85×10^{-7}
2°	formula	9.24×10^{-12}	6.08×10^{-9}	3.96×10^{-7}
4°	program	4.50×10^{-10}	2.73×10^{-7}	1.55×10^{-5}
4°	formula	3.52×10^{-10}	2.35×10^{-7}	1.57×10^{-5}

At the highest frequency and lowest temperature, the formula is off by a factor of 2. Otherwise the errors are no more than 30%.

Anomalous Skin Effect:

The preceding section assumes that the electron mean free path is small compared to the penetration depth, λ, so that the field acting on a given electron depends only on time. The anomalous skin effect occurs when this is not the case. We will make a crude estimate of this effect by considering electrons that are diffusely reflected from the surface and then travel a distance, l, before having a collisions. The electric field is approximated as being equal to its full value at depths up to λ, at which point it drops to zero. Figure 1 shows the effective mean free path, $L(\theta)$, for two such electrons. For $\theta > \cos^{-1}(\lambda/l) \sim \pi/2-\lambda/l$, the electron travels the full distance inside the penetration layer, so $L(\theta) = l$; for smaller angles, $L(\theta) = l/\cos(\theta)$.

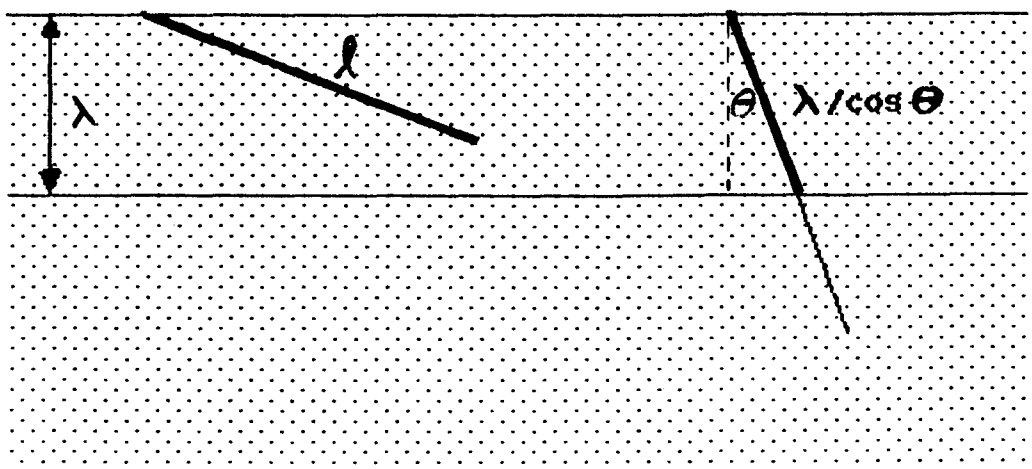

Figure 1. Effective mean free paths for $l > \xi$.

At low frequencies, the logarithm in [7] varies slowly with l, so that power loss is roughly proportional to l, as in equation [5]. The anomalous dissipation is then proportional to the average length,

$$l_{eff} = \frac{1}{4\pi} \int L(\theta)\, d\Omega$$

where θ is the angle between the electron trajectory and the normal to the surface, and $d\Omega = 2\pi \sin\theta\, d\theta$.

$$[8] \qquad l_{eff} = \int_{\pi/2-\lambda/l}^{\pi/2} l \sin\theta\, d\theta + \int_{0}^{\pi/2+-\lambda/l} \lambda \tan\theta\, d\theta = \lambda\,(\,1 + \log(l/\lambda)\,)$$

Most of the losses here are due to electrons traveling nearly parallel to the surface. If the mean free path is very long, then the low frequency approximation, $\omega < v_t/l$ is no longer valid. Since the

collision time is now longer than the RF period, further increases in l have little effect. For niobium at 4° these cutoff values for l are v_t/ω = 30,000 angstroms at 10 Ghz, or 600,000 angstroms at 0.5 Ghz. Figure 2, Taken from Martinez and Padamsee,{m4} shows surface resistance as a function of mean free path calculated with Halbritter's program.

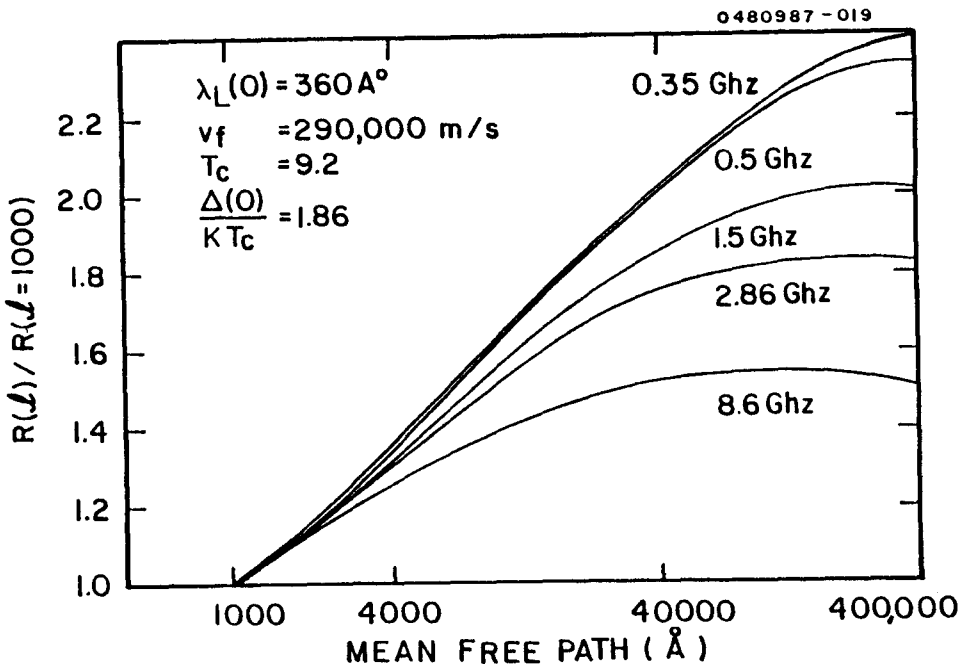

Figure 2. Calculated{m4} surface resistance of niobium as a function of mean free path for several frequencies.

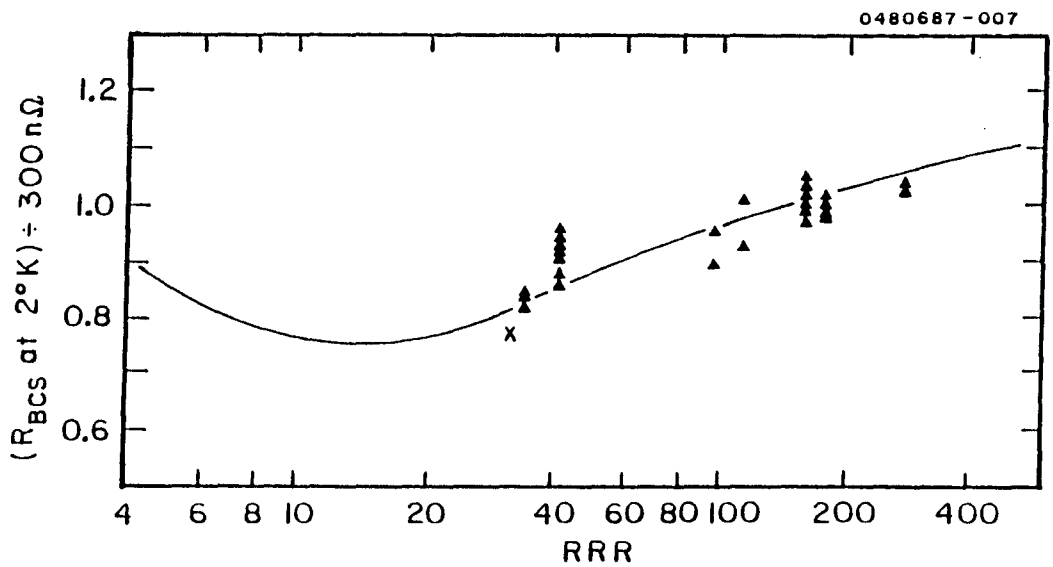

Figure 3. BCS resistance at 2°K and 8.6 Ghz as a function of niobium purity (RRR).

The logarithmic curve can be seen at low frequencies, and the upper limits are in approximately the right place. Formula [8] goes to zero at $1/\lambda = 1/e$. Extrapolating the straight line in figure 2 back to zero gives $\lambda = 120$ angstroms, which is off by about a factor of three, but not too bad considering the approximations that have been made. Of course [8] is not valid for $l < \lambda$. In fact, if $l < \xi$, both the normal current and the supercurrent are proportional to l, so that the surface resistance is proportional to $l^{-1/2}$. This results in a minimum in the surface resistance near $l = \xi$. Figure 3 shows this minimum in the curve, along with our data at 8.6 Ghz. The estimate $l = 20\text{Å}\cdot(RRR)$ has been used to relate the mean free path to the purity of the niobium.

2. Residual Resistance

The BCS theory predicts that the surface resistance of a superconductor goes to zero at T=0, but, in practice, this never happens. Instead the resistance approaches some finite value called the residual resistance. Common causes of residual resistance include contamination layers or inclusions of normal metal or lossy dielectrics, trapped magnetic flux, and cracks or splatters from welds. Other possible causes include damage from machining, surface roughness, grain boundaries, direct generation of phonons by the RF field, and oxide layers that have been damaged by heat or electron impact.{t1,t2,m3} Although many causes have been suggested or identified, there is little or no quantitative information about how much each of these mechanisms (with the exception of trapped magnetic flux{p3}) contributes to the residual resistance of a carefully prepared surface.

Resistive losses:

Probably the most common cause is the presence of normal conducting or lossy dielectric materials in the cavity. Even assuming that these losses are due to simple joule heating, $P = \text{Re}\,(\sigma|E|^2)/2$, there is a wide enough variety of possible behaviors that even this simple mechanism is hard to identify. Metallic materials cause higher losses if located in a high current region of the cavity. The frequency dependence of these losses depends on the size or thickness of the normal material. If the dimensions of the material are greater than its own skin depth, then the losses are proportional to $\omega^{-1/2}$. If the thickness is small compared to the penetration depth of the superconductor, then losses are proportional to $|E|^2$ at the surface of the superconductor, which varies as ω^2. Very small amounts of normal metals can cause significant losses. A typical S-band cavity that is uniformly coated with material having a resistivity of $1/\sigma = 1\ \mu\Omega$ cm should have a residual resistance of ~ 5 nΩ per angstrom of coverage.

An unresolved question is the extent to which thin surface layers will be driven superconducting by the proximity effect.{s1} The calculation of McMillan{m1} indicates that the surface layer will superconduct with an energy gap which is less than that of the superconducting substrate by a factor on the order of $(1-t/\xi)$, where ξ is the coherence length in the substrate. However, this calculation describes the energy spectrum of electrons that travel back and forth between the superconductor and the normal layer. Since--especially if there is an anomalous skin effect--significant losses are due to electrons travelling almost parallel to the surface, it remains unclear whether or not the proximity effect can eliminate the residual resistance of a normal layer.

Dielectric layers can cause losses in the high (perpendicular) electric field regions of the cavity. The displacement current, $J = -i\omega E/4\pi$, travels through this layer causing losses, $P = Re(|J|^2/2\sigma)$, where σ describes both the real current and the displacement current: $\sigma = \sigma_1 - i\omega\epsilon/4\pi$. The losses are then proportional to

$$Re(1/\sigma) = \sigma_1/(\sigma_1^2+\omega^2\epsilon^2/16\pi^2)$$

Note that the frequency dependence of these losses can vary between ω^2 and ω^0 depending on which part of the conductivity dominates.

Electron tunneling across cracks:

Another mechanism which might contribute to residual resistance is (single particle) tunneling across grain boundaries or cracks in the surface. Figure 4 shows an idealized crack with width, w, and depth, d. Most of the current detours around the bottom of the crack so that

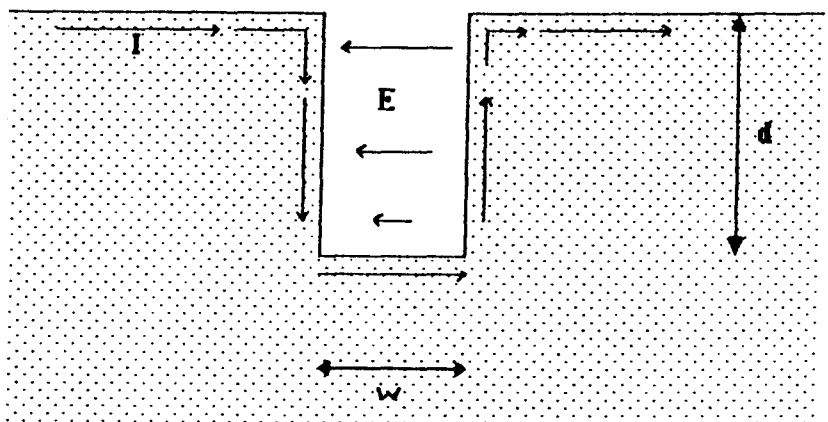

Figure 4. Idealized model of a crack in a cavity surface.

the magnetic field penetrates into the crack. The electric field then follows form the "curl E" equation so that the voltage across the crack is $V = wd(dB/dt)$ [mks units]. Significant tunneling will not occur unless $w < \sim 1000\text{Å}$, and the voltage is more than twice the energy gap, V

> ~ 3mV. Using a depth of 0.1mm and a frequency of 1 Ghz, we find that the RF magnetic field must reach ~300 gauss for tunneling losses to occur. (In a typical accelerator cavity, this corresponds to an accelerating field of ~10MV/m.)

The power dissipated by these junctions is probably small. For a given junction resistance, R, the current is (V-3mV)/R, and the power is VI = V(V-3mV)/R. A low estimate for R is $20\Omega\cdot[(1mm)^2/A]$ where A is the area of the junction. Since only the top portion of the crack has adequate voltage across it, the effective area is less than d times the length of the crack, so typical power losses are on the order of a few microwatts for a 1 cm long crack. This estimate is based on many speculative parameters, but, since almost any cavity will dissipate several watts at a field of 300 gauss, it seems unlikely that tunneling contributes significantly to these losses. Nonetheless, as Amato{a3} pointed out, this effect may be observable since the nonlinear conductivity of the junctions should generate third harmonics of the resonant frequency.

Direct phonon generation:

Direct generation of phonons by RF electric fields has been investigated by several authors {h3,p2,k3,s2} as a possible cause of residual resistance. The most recent calculations, due to Scharnberg, find less than one nΩ for frequencies less than 4 Ghz. However, for higher frequencies and relatively long mean free paths (>1000A), the results become comparable with experimental values. Figure 5 shows residual resistance as a function of RRR for the UHV fired cavities

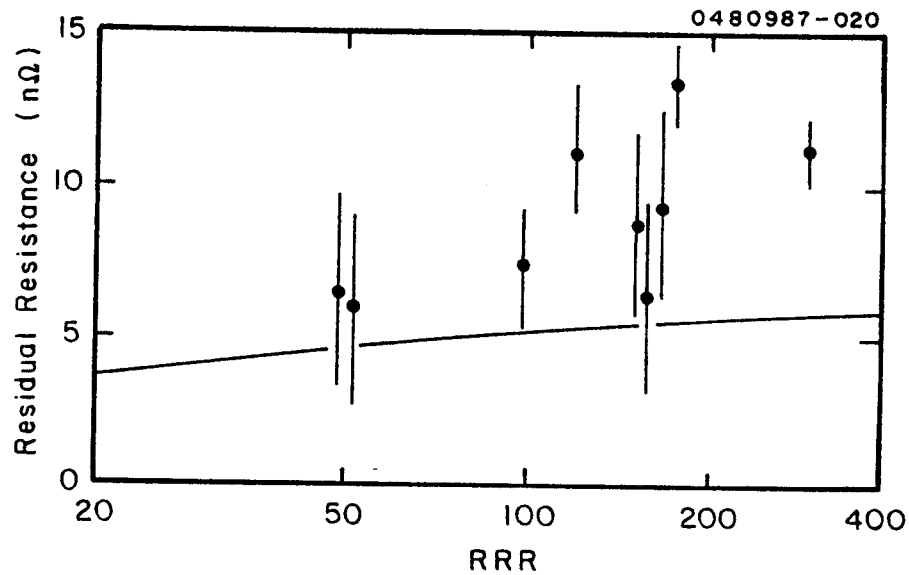

Figure 5. Residual resistance of niobium at 8.6 Ghz as a function of niobium purity (RRR).

described below. The curve through the figure is interpolated from Scharnberg's graphs. Although the data is not completely convincing, it should be interesting to see if other researchers find an increase in high-frequency surface resistance with RRR.

3. Effects of Oxygen

Oxide layers have long been suspected of contributing to residual resistance. Niobium oxidizes quickly in air, forming an oxide layer that grows to 10 - 15 Å in a few seconds, and then grows more slowly, reaching a thickness of 50 100 Å after many days. XPS studies{g1,k1} have shown that this layer consists mostly of an oxide which has roughly the same stoichiometry as Nb_2O_5. There may be an interface layer of lower oxides between the pentoxide and the metal, but this interface is so thin that the XPS data cannot be unambiguously interpreted. Possible contributors to residual resistance include NbO, which (if present) behaves like a normal metal with a transition temperature of ~1.3°{h2}, and Nb_2O_5, which may become a lossy dielectric if it deviates from stoichiometry.{g2}

The principal goal of our recent research{p5} has been to measure the influence of oxide layers on the residual resistance of niobium by comparing the surface resistance of oxidized and oxide-free surfaces. A

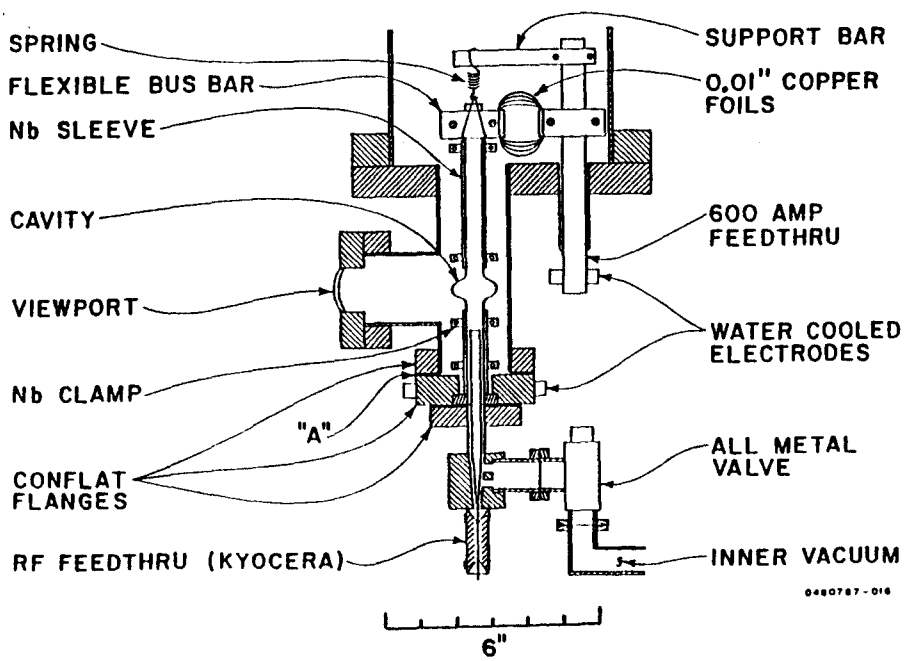

Figure 6. Ultra-high-vacuum furnace used to remove oxide layers from inner surface of cavities.

procedure for cleaning the niobium was developed based on studies in the literature{f1} and on our own Auger measurements.{p4} The native oxide layer was removed from the surface by heating to 1100°C for 20 minutes. At this temperature, the oxygen was absorbed into the bulk; however, sulfur sometimes precipitated to the surface at the same time. The sulfur was removed by heating to 1400° for one minute.

Figure 6 shows the ultra high vacuum furnace used to heat cavities to these temperatures. A current of up to 350 amps passes through the feedthrough and the flexible bus bar, down the top cutoff tube, through the cavity and the lower cutoff tube, and out through the cavity flange. The 0.062" thick niobium sleeves around both cutoff tubes conduct heat and electricity so that the cavity becomes the hottest part of the furnace. The spring-supported flexible bus bar keeps the cavity from being crushed by thermal expansion. After firing, the seal was broken at "A" (fig.6), the all metal valve was closed, and the cavity was taken to the cryostat for testing. Transfer from the furnace to the cryostat took about an hour.

Room temperature exposure:

The first group of measurements were done in order to determine the influence of oxide layers on residual resistance. Cavities were UHV fired at T > 1100°C in order to remove the oxide layer, and then repeatedly exposed, first to argon as a control, and then to oxygen. Each pair of exposures was of greater duration and/or pressure than the preceding pair; and each exposure, as well as the initial firing, was followed by a cryotest. The results are shown in Table 2. With the

TABLE 2

Residual resistance as a function of successive surface treatment

Run#	Surface Condition	Residual Resistance	RRR
	Cavity # 2		
9	BCP, Fired @ 1400C	6.2 n-ohms	42
10	Exposed .02 torr Ar for 2 min.	5.9	"
11	.02 torr O - 2min	8.4	"
12	.1 torr Ar - 1hr	7.5	"
13	(same as 12 - retest)	9.6	"
15	.1 torr O - 1hr	7.1	"
16	.1 toor O - 45hr	21.2 (leaked?)	"
	Cavity # 4		
19	BCP, Fired @ 1400C	7.6	160
20	.1 torr Ar - 16hr	5.8	"
22	.1 torr O - 16hr	7.7	"
23	.1 torr Ar - 48hr	8.6	"
24	.1 torr O - 48hr	7.3	"

exception of one measurement, there is no evidence of any change. There is good reason to suspect that the high value obtained on run 16 was due to a leak in the cavity. On the next test, after chemical polishing and firing, this cavity exhibited strange nonexponential decay curves. A few thermal cycles later, a leak was found with a helium leak detector.

In order to find an upper bound for the influence of oxygen exposure on residual resistance, we have compared the residual resistance of all the fired cavities before and after their first exposure to oxygen. These data are shown in Table 3. Wherever multiple measurements are available, their average (weighted $1/\sigma^2$) is used. Our final conclusion is that these oxide layers contribute less than 1.5 nΩ to the residual resistance.

Table 3

Change in R_{res} after first exposure to O_2

Run #'s Unexposed	Run #'s Exposed	Exposure to Oxygen	Change (nΩ)
9,10	11	1 min. at 0.02 torr	+2.4 ± 2.6
19,20,21	22	16 hr. at 0.1 torr	+0.6 ± 3.0
32,33	34	16 hr. at 0.2 torr	+1.1 ± 2.0
45,47,48	55	2 hr. at 0.1 torr	-1.1 ± 1.7
60	64	2 hr. at 0.15 torr	-1.9 ± 2.1
Average (weighted: $1/\sigma^2$)			-0.1 ± 1.5

Surface resistance of cavities heated to 325°C:

Upon finding that exposure to oxygen did not affect the RF performance of the cleaned cavities, it became necessary to make sure that the cleaned cavities were actually oxide-free. Although Auger measurements{p4} showed that most of the native oxide was absorbed at 1100°, it was hard to assess the contamination that occurred in between the cooldown from T > 1000°, and the cryotest. The technique of heating the (evacuated) cavities to 325°C for 10 minutes was developed to get around this problem. At this temperature, the surface oxides decompose, and the oxygen diffuses into the metal, creating an oxygen-rich layer which is a few thousand angstroms thick. These layers showed a reduced BCS resistance and an increased residual resistance, which provided an indirect measurement of the thickness of the original surface oxides.

Three cycles of measurements were made to compare the surface resistance of oxidized and unoxidized cavities, which had been heated in this manner. Each cycle consisted of the following surface treatments, with a cryotest following each treatment: buffer chemical polish and rinsing, oxide removal by firing at 1200 - 1400°C, heating to 325° for 10 minutes, exposure to 0.1 torr oxygen for 2 to 16 hours (the time doesn't seem to matter), and reheating to 325°. The unoxidized cavities were sometimes heated twice in order to collect additional data.

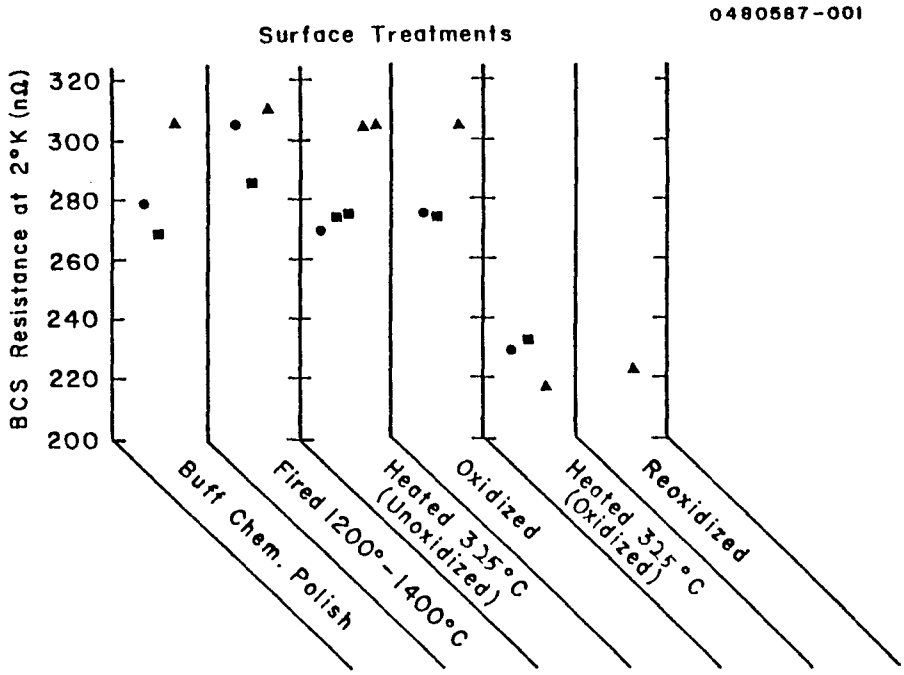

Figure 7. BCS resistance at 2°K as a function of successive surface treatments. o: cavity 4 runs 31 through 37, □: cavity 4 runs 38 through 43, Δ: cavity 6 runs 44 through 58.

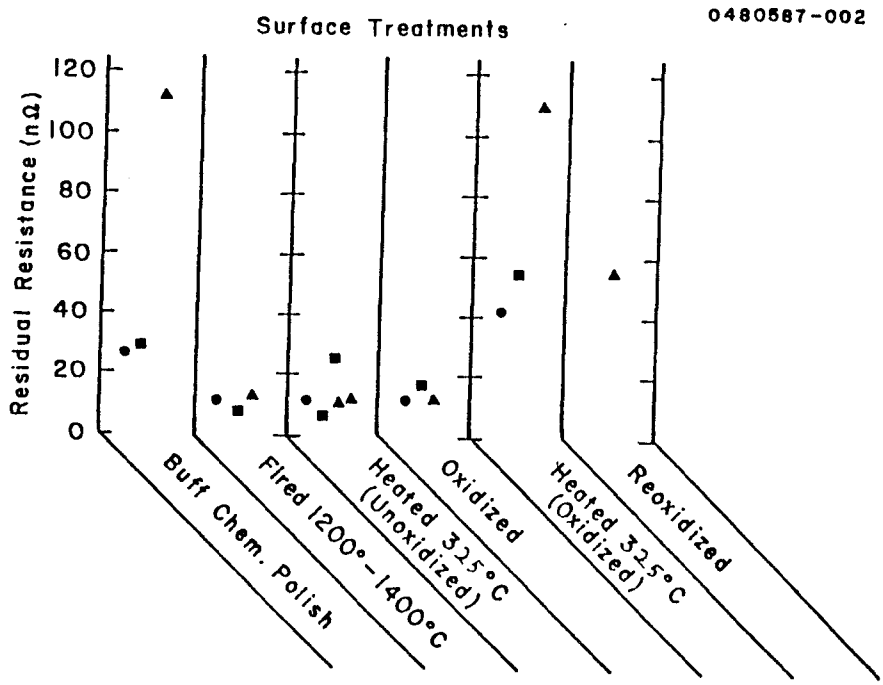

Figure 8. Residual resistance as a function of successive surface treatments for the same cavities shown in figure 7.

Figures 7 and 8 show the effects of these treatments on the BCS resistance at 2°K, and on the residual resistance. When oxidized surfaces are heated to 325°C, the BCS resistance decreases by about 20%, but the residual resistance increases by about 50 nΩ. These two effects cancel each other near 2 degrees . The oxide-free cavities were usually not affected by this heating. Since the oxidized cavities cavities were probably covered with about 15 angstroms of Nb_2O_5, this implies that oxygen contamination of the UHV fired surfaces probably does not exceed one or two monolayers.

The last column of figure 8 shows a single measurement in which a final exposure to oxygen reduced the residual resistance of a cavity which had been first oxidized and then heated. This might suggest that the residual resistance of the heated cavity was due to a layer of suboxides that was then converted to the dielectric, Nb_2O_5, by exposure to oxygen. However, no such layer was found by Kirby et al., using XPS measurements.{k6}

Energy Gap:

It is surprising that no significant variations in the energy gap were observed. It is well known{d1} that dissolved oxygen lowers the critical temperature of niobium by ~1° per atomic percent (which was observed), and that the BCS theory predicts that the energy gap is

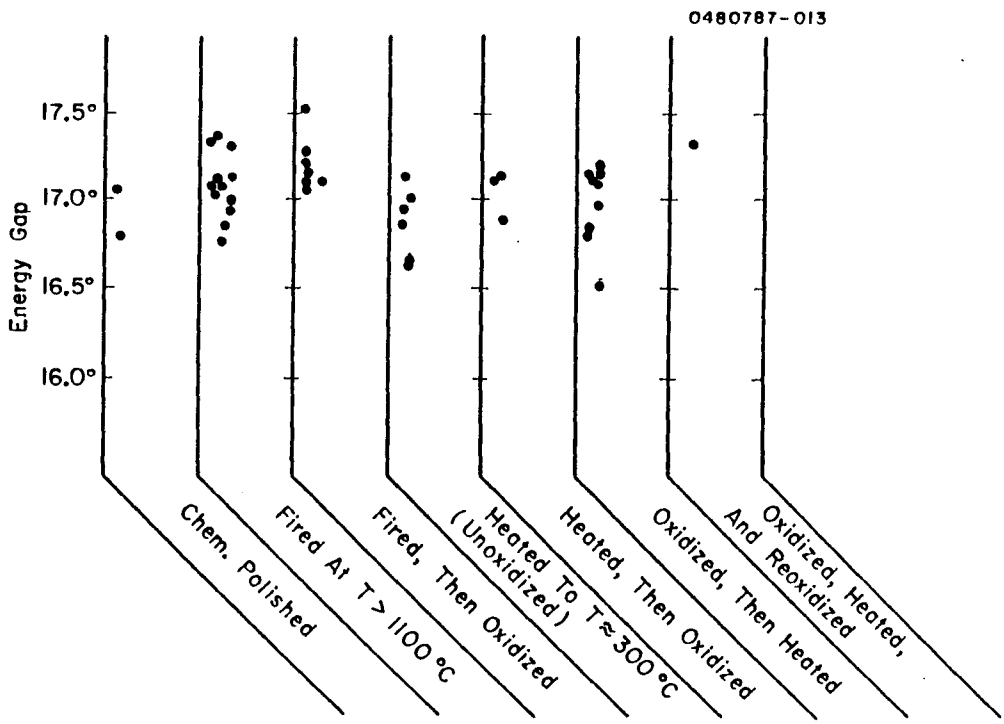

Figure 9. Energy gap for cavities with various surface treatments (error bars not shown).

related to the critical temperature by $\Delta = 1.76\ T_c$. Furthermore, variations in the gap have been reported under similar circumstances{p6}.

Figure 9 shows gap values grouped according to surface preparation of the cavities. Note that there are two groups of data for each heat treatment, depending on whether or not the cavity had been exposed to oxygen after the treatment. Figure 10 shows the mean and the error in the mean for each heat treatment. The various heat treatments alter the energy gap by less than 1 percent.

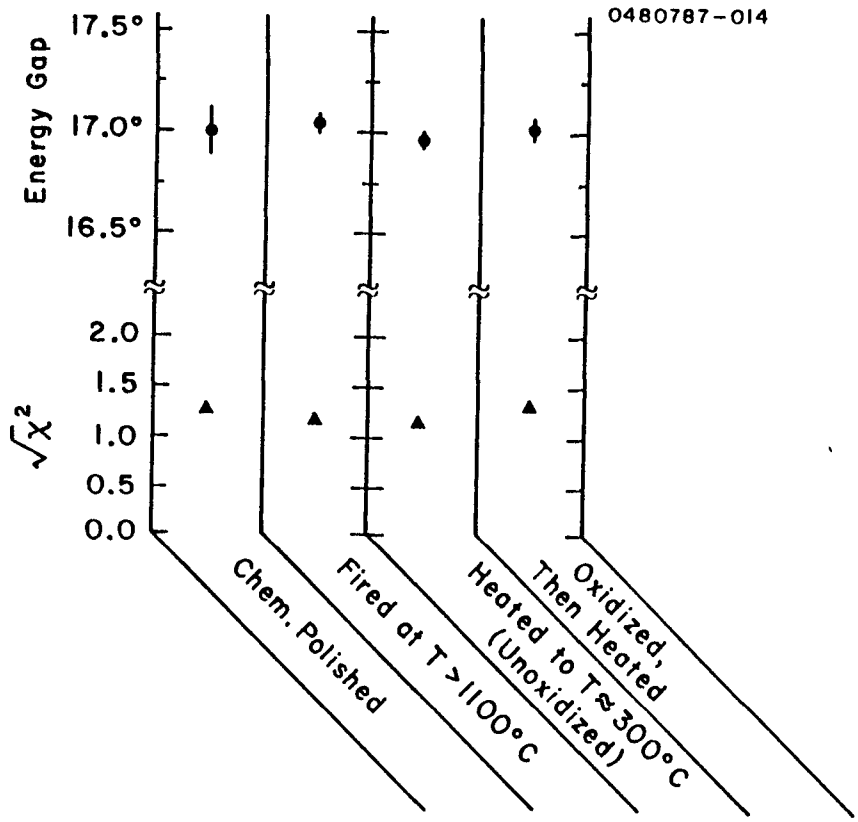

Figure 10. Average energy gap for the heat treatments shown in figure 9.

Although no change in the gap was observed, heating an oxidized cavity did reduce its RF transition temperature (T_c) by a few tenths of a degree. The significance of these data are somewhat unclear since the influences of concentration gradients and proximity effects are not known, but it does seem safe to assume that RF measurements sample a depth no greater than the normal skin depth, which, in this case, is equal to $2\ \mu m/(RRR)^{1/2}$, where RRR is the local residual resistivity ratio.

The RF transitions for several cavities are shown in figure 11. All of the cavities which were oxidized and heated have T_c values below 9°. Two of these cavities were then chemical polished to remove the oxygen-rich layer, after which the T_c was remeasured. These pairs of points are indicated by identically shaped data points. Several other chemical polished or heated cavities are indicated by round dots. The temperature calibration may contain an offset of one or two tenths of a degree, but the changes in temperature should be within the error bars shown. It was necessary to expose the cavities to air in order to make these measurements.

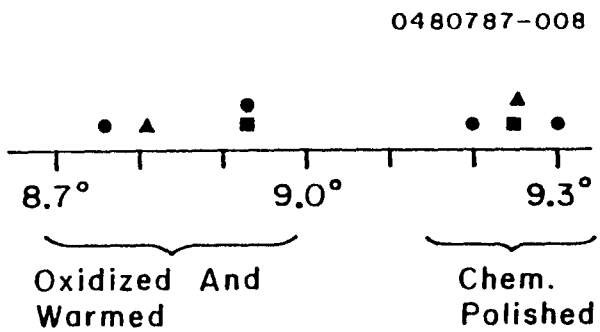

Figure 11. RF transition temperatures for several cavities after oxidation and heating to temperatures near 300°C, and after chemical polishing. □: Cavity #4 after run 43. Δ: Cavity #6 after run 58. o: Other cavities.

Dependence of RF properties on heating temperature:

A single cycle of measurements was made in order to determine the effects of heating to different temperatures. While the reproducibility of single measurements has not been checked, at least some of the trends in the data are probably correct. The cavity was first cold polished and fired, then oxidized, and then heated to successively higher temperatures with a cryotest following each of these procedures. Figure 12 A and 12 B show the BCS resistance at 2 degrees, and the residual resistance after firing and oxidation, and after heating to three successive temperatures. The BCS resistance declines upon heating to 250°C, rises almost back to its original value at 280°, and then falls again at 350°. At some still higher temperature, the heating will make the surface oxygen-free, and the BCS resistance should return to its original value. The residual resistance has only a single peak at around 280°.

Bob Kirby et al.{k6} have done an XPS study of the behavior of oxidized niobium near 300°. The samples, which had RRR values between 100 and 200, were UHV fired in the same manner as these cavities and exposed to 0.1 torr of oxygen for 2 hours. XPS measurements were then taken while the niobium was slowly heated to 375° over a period of 20

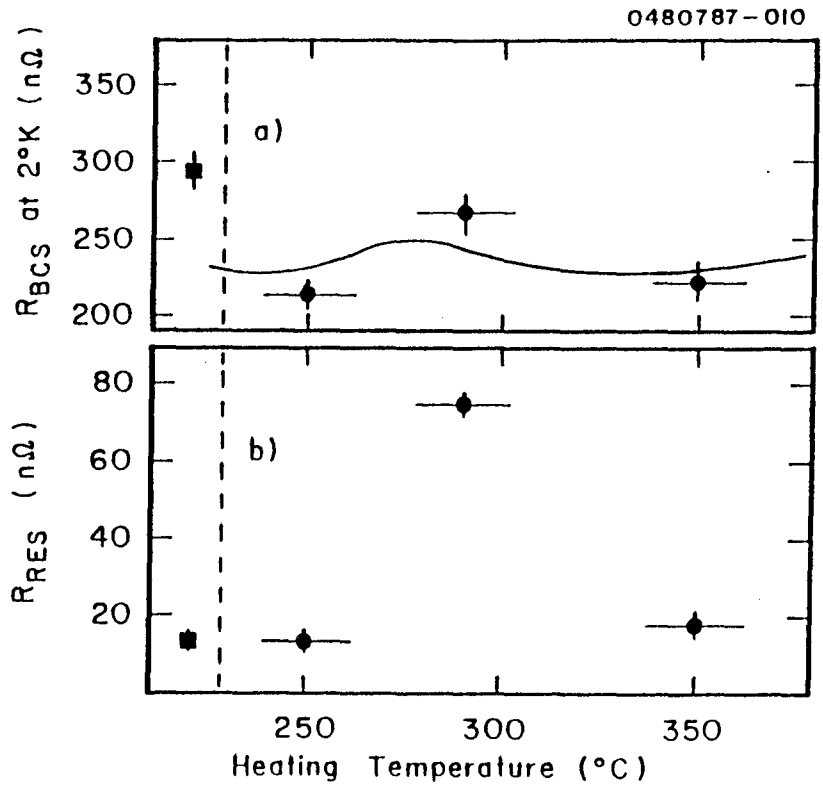

Figure 12. BCS resistance at 2°K (A), and residual resistance (B) for an oxidized niobium cavity after heating in vacuum to successively higher temperatures. Square points show values prior to oxidation.

minutes. Their results may be summarized as follows. Before heating, the niobium is covered with about 13 angstroms of Nb_2O_5; no other oxides could be detected with certainty. Between 100° and 200°, the Nb_2O_5 begins to break up into oxides with nearly the same stoichiometry, such as NbO_2, but most or all of the oxygen remains within ~20 angstroms of the surface. At around 250°, the oxygen begins to dissolve into the nearby bulk metal, and by 300°, the oxide layer is almost completely gone. At no point in time was any significant amount of lower oxides such as NbO observed.

The curve through 12A was calculated based on these XPS results and on the diffusion equation, which governs the motion of dissolved oxygen moving through niobium metal: {p1}

$$\frac{\partial c}{\partial t} = D(T) \frac{\partial^2 c}{\partial x^2}$$

where c is the oxygen concentration, x is the distance from the surface, and D is the diffusion constant, which depends only on the (Kelvin) temperature.

$$D(T) = 0.02 \cdot \exp\left(\frac{13500}{T}\right) \left(\frac{cm^2}{sec}\right)$$

A particularly useful solution to the diffusion equation is

[9] $$c = \frac{A}{\delta \sqrt{\pi}} \exp\left(\frac{-x^2}{4\delta^2}\right)$$

where δ^2 is the time integral of the diffusion constant, $\int D\, dt$; and A is the total amount of oxygen per unit area, $\int_0^\infty c\, dx$.
This solution describes an oxygen profile that begins as a delta function at the surface. At 250° or more, the diffusion length (δ) grows to more than the superconducting penetration depth (~350 angstroms) in only a few seconds, so the prefactor, $A/\delta\sqrt{\pi}$, gives the concentration in the region of interest. Note also that the diffusion constant increases so rapidly with temperature that the results for the cumulative heatings shown in figure 12A are nearly the same as the result for a single heating at the indicated temperature. The curve through figure 12A was calculated using Halbritters program (fig. 3) and the concentration from [9]. δ was calculated using a time of 200 seconds at the indicated temperature (allowing 100 sec. for the oxides to break up and begin to dissolve); and A was found by assuming that the initial layer of Nb_2O_5 was 13 angstroms thick, and the fraction, f, of that layer which dissolves at a given temperature is given by the fermi-type function,

$$f = \frac{1}{1 + \exp\left(\frac{265°C - T}{15°}\right)}$$

which is in reasonable agreement with the XPS measurements. The curve fits the data well enough to believe that the general explanations given here may be correct.

Trapped magnetic flux:

One of the most thoroughly documented{p3} causes of residual resistance is magnetic flux which is traped in the cavity walls during cooldown through the critical temperature. A theory for type II materials{g3}, based on the motion of flux lines in the metal, predicts a residual resistance of roughly $R_{res} = R_n(B/H_{c2})$, where R_n is the normal surface resaistance, and B is the magnetic flux density penetrating the superconductor. This value is in tolerable agreement with experiment, however, in many cases of practical interest the problem is more complicated, due at least in part to the difficulty of determining the fraction of the ambient field that actually is trapped in the cavity walls. For example, Lyenis{l1} found that the

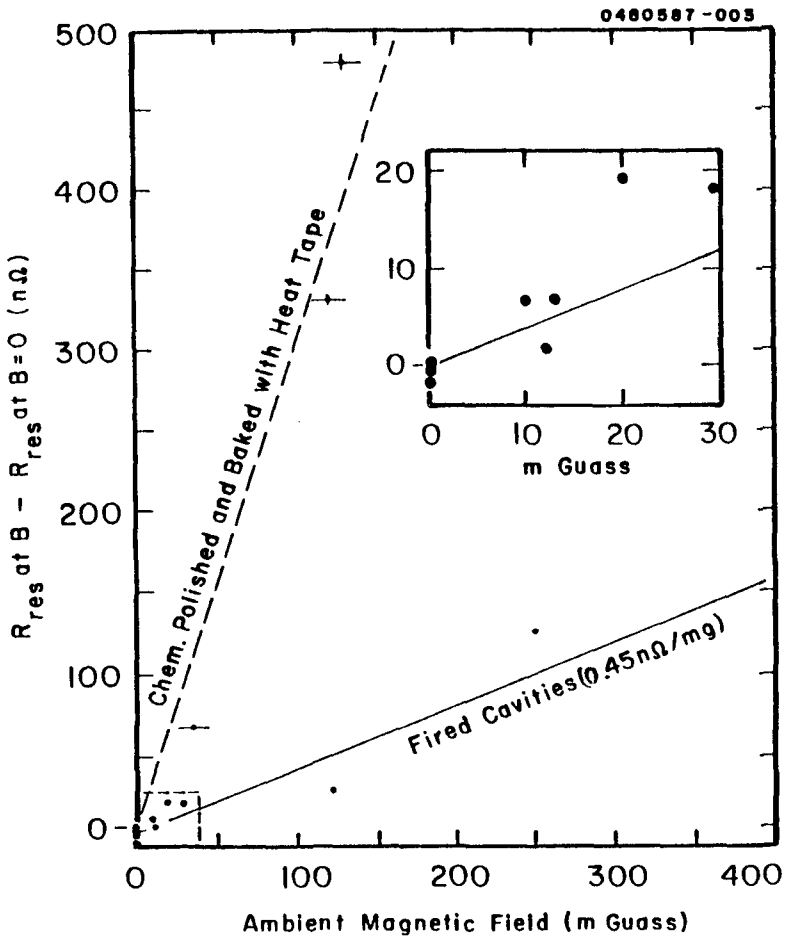

Figure 13. Increase in residual resistance due to ambient magnetic field applied during cooldown. Inset shows points near origin.

residual resistance could be reduced by an order of magnitude if the cavities were cooled very slowly (~10^{-3} deg/min) through the transition temperature, while niobium-sputtered copper cavities at CERN{a1} show no field-induced residual resistance at all.

Figure 13 shows residual resistance of two different cavities as a function of ambient magnetic field during cooldown. The results are only reproducible to about ± 40%, but they show two distinct curves, both of which are roughly linear. The lower curve, with a slope between 0.3 and 0.6 nΩ/milligauss, was measured on a cavity which had an RRR of 280 and an oxide free (fired) surface. The upper curve, with a slope of about 3 nΩ/milligauss, was measured on a cavity cavity with an RRR of about 100, which had been chemical polished, rinsed, and then evacuated and baked overnight at an unknown temperature (maybe 200°C).

Kneisel et al.{k3} observed a similar phenomenon on niobium cylinders which had been cooled to room temperature very slowly (~12 hr.) after UHV Firing. Residual oxygen or CO in the furnace presumably contaminated the cavity surface during this cooldown. The effective penetration depth measured as a function of DC magnetic field, showed an irreversibility due to trapped flux. This effect was much smaller on samples that had been cooled roughly three times faster.

REFERENCES

a1 B. Arnolds-Meyer and W. Weingarten, "Comparative Measurements on Niobium Sheet and Sputter Coated Cavities," IEEE Trans. Mag. MAG-23, 1620 (1987).

a2 A. Abrikosov, L. Gorkov, and I. Khalatnikov, "A Superconductor in a High Frequency Field," Soviet Phys. JETP 8, 182, (1959).

a3 J. Amato, comment during question period for this paper.

d1 W. DeSorbo, "Effect of Dissolved gases on some Superconducting Properties of Niobium," Phys. Rev. 132, 107 (1963).

f1 H. Farrell, H Isaacs, and M. Strongin,"The Interaction of Oxygen and Nitrogen with the Niobium (100) Surface II," Surf. Sci. 38, 31 (1973).

g1 M. Grundner and J. Halbritter, "XPS and AES Studies on Oxide Growth and Oxide Coatings on Niobium," F. Appl. Phys. 51, 397 (1980).

g2 E. Greener, D. Whitmore, and M. Fine, "Electrical conductivity of Near Stoichiometric α-Nb_2O_5," J. Chem. Phys. 34, 1017 (1969).

g3 J. Gilchrist "Microwave Surface Resistance of Type II Superconductors," Proc. Roy. Soc. A295, 399 (1966).

h1 J. Halbritter, "Comparison between measured and calculated RF losses in the Superconducting State," Z. Physik 238, 466 (1970).

h2 J. Hulm, C. Jones, R. Hein, and J. Gibson, "Superconductivity in the Ti-O and Nb-O Systems," J. Low Temp. Phys. 7, 291 (1972).

h3 J. Halbritter, J. Appl. Phys. 42, 82 (1971).

k1 P. Karulkar and J. Nordman, "Study of Thin Nb Oxide Films," J. Vac. Sci. Tech. 17 262 (1980).

k2 P. Kneisel, O. Stoltz, and J. Halbritter, "On Surface Preparation and Measurement of Niobium Used in High Frequency Cavities," J. Appl. Phys. 45, 2296 (1974).

k3 E. Kartheuser and S. Rodriguez, "Effect of Acoustic Generation on the Residual Surface Impedence of Superconductors," J. Appl. Phys. 47, 700 (1976).

k4 P. Kneisel, O. Stoltz, and J. Halbritter, "Investigation of the Surface Resistance of a Niobium Cavity at S-Band," IEEE Trans. Nuc. Sci. NS-18, 158 (1971).

k5 P. Kneisel, "Surface Preparation of Niobium," Proceedings of the Workshop on RF Superconductivity, M. Kuntze ed., 27 (Kernforschungszentrum Karlsruhe, 1980).

k6 R. Kirby, F. Palmer, E. Garwin, F. King, and M. Tigner, to be published.

l1 C. Lyenis, Thesis, Stanford University, Stanford, California, (1974).

m1 W. McMillan, "Tunneling Model of the Superconducting Proximity Effect," Phys. Rev. 175, 573 (1968).

m2 D. Mattis and J. Bardeen, "Theory of the Anomalous Skin Effect in Normal and Superconducting Metals," Phys. Rev. 111, 412 (1958).

m3 G. Muller, "Diagnostic Techniques and Defect Classification," Proceedings of the Second Workshop on RF Superconductivity, H. Lengeler, ed., 377 (CERN, Geneva, 1984).

p1 R. Powers and M. Doyle, "Diffusion of Interstitial Solutes in Group 5 Transition Metals," J. Appl. Phys., 30, 514 (1959).

p2 C. Passow, "Explanation of the Low-Temperature High-Frequency Residual Surface Resistance of Superconductors," Phys. Rev. Let. 28, 427 (1972).

p3 J. Pierce, "Superconducting Microwave resonators" in Methods of Experimental Physics, Vol. 2, R. Coleman, ed. (Academic Press, N.Y.,1974).

p4 F. Palmer and M. Tigner, "Effect of Oxide Layer on Microwave Surface Resistance of Superconductiong Niobium,"IEEE Trans. Mag., MAG 21, 1011 (1985).

p5 F. Palmer, "Influence of Oxide Layers on the Microwave Surface Resistnace of Niobium," IEEE Trans. Mag MAG-23, (1987).

p6 A. Phillip and J. Halbritter, "Investigation of the Gap Edge Density of States at Oxidized Niobium Surfaces by RF measurements," IEEE Trans. Mag. Mag-19, 999 (1983).

s1 M. Strongin, "The Sensitivity of the Q of Superconducting RF Cavities to Surface Conditions," J. Appl. Phys. 42, 4105 (1971).

s2 K. Scharnberg, "Comment on the Residual RF Surface Resistance of Superconductors," J. Appl. Phys. 48, 3462 (1977).

t1 J. Turneaure, "Status of Superconductivity for RF Applications," Proceedings of the 1972 Applied Superconductivity Conference, IEEE Pub. No. 72CHO682-TABSC, 621 (1972)

t2 M. Tigner and H Padamsee, "Superconducting Microwave Cavities in Accelerators for Particle Physics--A Review," in Physics of High Energy Particle Accelerators, SLAC Summer School--1982, M. Month, ed., AIP Conf. Proc. 105, 801 (1983).